J Membrane Biol (2015) 248:497–503
DOI 10.1007/s00232-015-9807-8

Insights from Micro-second Atomistic Simulations of Melittin in Thin Lipid Bilayers

Sanjay K. Upadhyay[1] · Yukun Wang[2] · Tangzhen Zhao[1] · Jakob P. Ulmschneider[1]

Received: 20 January 2015 / Accepted: 4 May 2015 / Published online: 12 May 2015

Abstract The membrane disruption and pore-forming mechanism of melittin has been widely explored by experiments and computational studies. However, the precise mechanism is still enigmatic, and further study is required to turn antimicrobial peptides into future promising drugs against microbes. In this study, unbiased microsecond (μs) time scale (total 17 μs) atomistic molecular dynamics simulation were performed on multiple melittin systems in 1,2-dimyristoyl-sn-glycero-3-phosphocholine membrane to capture the various events during the membrane disorder produced by melittin. We observed bent U-shaped conformations of melittin, penetrated deeply into the membrane in all simulations, and a special double U-shaped structure. However, no peptide transmembrane insertion, nor pore formation was seen, indicating that these processes occur on much longer timescales, and suggesting that many prior computational studies of melittin were not sufficiently unbiased.

Keywords Antimicrobial peptides · Melittin · Lipid bilayer membranes · Molecular dynamics simulations

Electronic supplementary material The online version of this article (doi:10.1007/s00232-015-9807-8) contains supplementary material, which is available to authorized users.

✉ Jakob P. Ulmschneider
jakobulmschneider@hotmail.com; jakob@sjtu.edu.cn

[1] Institute of Natural Sciences and Department of Physics and Astronomy, Shanghai Jiao Tong University, Shanghai 200240, China

[2] The State Key Laboratory of Microbial Metabolism and College of Life Sciences and Biotechnology, Shanghai Jiao Tong University, Shanghai 200240, China

Introduction

Antimicrobial peptides (AMPs) are small proteins (10–50 amino acids) with a majority of hydrophobic residues in combination with a few positively charged residues lining one side. Two important characteristics of AMPs are attractive to consider them as future promising drugs against multi-drug-resistant microbes. One, they have a wide range of activity against both gram-positive and gram-negative bacteria as well as fungi, viruses, and mycobacteria (Brogden 2005; Chromek et al. 2006; Hancock and Scott 2000; Son et al. 2007). Two, they interact directly with cell membranes rather than with specific receptor proteins, and thus are potentially free from antibiotic resistance developed by microbes (Lohner and Blondelle 2005). It is well known that the membrane disruptive properties of AMPs are involved in the killing of microorganisms and several models, such as barrel-stave (Langham et al. 2008; Lohner and Blondelle 2005; Park and Hahm 2005; Sanchez-Martinez et al. 2008; Yang et al. 2001), toroidal pore (Allende et al. 2005; Hancock and Scott 2000; Lohner and Blondelle 2005; Matsuzaki et al. 1997; Park and Hahm 2005; Sharon et al. 1999; Yang et al. 2001) and carpet models (Brogden 2005; Brown and Hancock 2006; Lohner and Blondelle 2005; Yeaman and Yount 2003) have been proposed to explain the action of AMPs. However, none of them are able to describe all the experimental observations. Therefore, understanding the mechanism of membrane permeabilization of AMPs in detail is essential for the development of AMPs into full-fledged antimicrobial drugs. The focus of the current study is restricted to melittin, which has been extensively studied by both experimental and simulation methods. Melittin is a 26-residue-long peptide that has been reported to have anticancer, antiviral, antibacterial, anti-arthritis, and hemolytic effects.

The C-terminus of the peptide is strongly cationic in nature with four positively charged residues (Lys-Arg-Lys-Arg), while the rest (residues 1–20) are mostly hydrophobic in nature with only two positive charges that are located at Lys-7 and the N-terminus.

Several experimental studies suggest that the action of melittin on bilayers depends on experimental conditions such as the composition of the membrane, temperature, pH, and the concentration of the peptides (Brown et al. 1980; Iwadate et al. 1998; Zhu et al. 1995). Originally, it was proposed that at higher concentration, melittin may disrupt bilayer through the carpet mechanism. Later, several experimental and simulation studies suggested that the formation of barrel-stave or toroidal-shaped pores might be responsible for leakage and disturbance of membranes. The pore-forming propensity of melittin depends on lipid/peptide ratio (Demchenko and Kostrzhevskaia 1986; Lee et al. 2013; van den Bogaart et al. 2008). At low concentrations, melittin lies parallel to the membrane surface and inserts itself into a transmembrane orientation (TM) when the concentration reaches above threshold. The inter-conversion of these two states is possible at equilibrium conditions and might be directly associated with lytic activity (Brogden 2005; Chen et al. 2007). However, another study revealed that since melittin carries high cationic (+5) charges at neutral pH, and interacts strongly with the lipid head groups, the reorientation from parallel to TM is very expensive in terms of energy and may not be feasible (Huang 2000; Manna and Mukhopadhyay 2009). In another study, it is proposed that the orientation of peptides in either conformation is concentration dependent and competing with each other. Thus, the parallel binding to membrane by melittin actually competes with the peptide insertion and the pore formation (van den Bogaart et al. 2008). Previous MD simulations of melittin have shown that when adsorbed on the bilayer surface, melittin affects both leaflets of the membrane causing thinning of the upper layer, which in turn favors water penetration through the lower layer (Berneche et al. 1998). Another MD study showed spontaneous pore formation by melittin and concluded that the aggregation of peptides above the threshold concentration on membrane surface is the pre-condition for pore formation (Sengupta et al. 2008).

Manna and Mukhopadhyay (2009) reported an ion-permeable toroidal pore within 15 ns MD simulation using pre-assembled four melittin peptides in TM orientation. The N-terminus of the peptides was located in the lipid bilayers in TM orientations that pulled some water from the lower leaflet of the membrane and resembled a toroidal pore. Another atomistic simulation study discussed the influence of secondary structures and arrangement of melittin on the bilayer, and concluded that the less helical and symmetric arrangement of melittin on both the surfaces of bilayer favored the toroidal pore formation (Irudayam and Berkowitz 2011). In a consecutive study, they concluded that the binding of melittin on the bilayer is a two-step process; first it absorbed parallel to the bilayer surface followed by reorientation to adopt a shallow U-shaped structure parallel to the membrane normal (Irudayam and Berkowitz 2012). The reorientation required higher concentration of peptides which induced membrane thinning and facilitated pore formation. Recently, Santo et al. (Santo et al. 2013) performed a coarse-grained (CG) simulation using MARTINI force field for a μs time scale and observed transient pore formation by melittin. They concluded that the pore formed when 3–5 peptides assembled together and it was not essential to reorient all the peptides normal to the membrane surface; many of them had their terminal residues anchored to the same leaflet, and these peptides assumed bent, U-shaped conformations.

Although large number of studies have been carried out to understand the mechanism of pore formation or membrane disruption by melittin, the exact mechanism by which melittin disrupts membranes is still mysterious. All the atomistic MD simulations for melittin were carried out either for nanosecond (ns) time scales, and in the form of artificially created pre-pore conditions. Instead, unbiased, longer time scale atomistic simulations are required to address the ambiguity in the membrane disruption mechanism. We have performed a total of 17 μs unbiased atomistic simulation to understand the mechanism of membrane disturbance by melittin. In this paper, the implication of these results and their impact on membrane stability will be discussed.

Methods

System Preparation

We performed a total of five simulations of melittin (GIGAVLKVLTTGLPALISWIKRKRQQ) within a lipid bilayer of 1,2-dimyristoyl-sn-glycero-3-phosphocholine (DMPC). The pore formation by melittin depends on several parameters, the most important of which is the *P*/*L* ratio. Unfortunately, it is controversial at what exact *P*/*L* ratio pores are supposed to form. In several studies, it is reported that melittin induces pore formation only when the threshold ratio between peptide/lipids (*P*/*L*) is below 1:60 (Lee et al. 2013; van den Bogaart et al. 2008; Vogel and Jahnig 1986). In contrast, others (Rex 1996; Schwarz et al. 1992) observed dye leakage and pore formation at much lower *P*/*L* ratio (*P*/*L* > 1:200). To be sure we have enough peptide, we chose *P*/*L* ratios far away from those critical ratios. Coordinates of melittin were retrieved from the protein data bank (PDB ID: 2MLT) in α-helical

conformation (www.rcsb.org). Initially, two systems were set up with *P*/*L* ratio 1:30, one each in symmetric (one peptide at each leaflet of the membrane) and asymmetric conditions (both peptides in the same leaflet of the membrane). In both cases, peptides were located randomly above the lipid–water interface, with no initial interaction between the lipid head groups and peptides. This arrangement made the systems unbiased from any pre-imposed conditions. The systems were then minimized and 50 ns MD was run for each system. Within these time scales, the peptides randomly interacted with the lipid head groups parallel to the membrane surface. At this stage, we extracted the last frame from the simulations and removed five lipids from each leaflet. The removal of the lipids was sequential and every time required 5–10-ns equilibration. Thus, the final system was with *P*/*L* ratio 1:25. A similar procedure was used for the setup of big systems in both symmetric and asymmetric conditions (total eight peptides within 200 DMPC lipids). Another system with *P*/*L* ratio 1:23 (total 18 peptides within 418 DMPC lipids) was setup, where nine peptides were partially inserted into the membrane and others remained parallel to the membrane surface. The inserted peptides were placed at equal distances to eliminate any biasness such as pre-pore conditions lined with several peptides or any type of preliminary interaction between the peptides that could assist in peptide aggregations. A summary of simulated systems is listed in Table 1.

Simulation Parameters

MD Simulations were performed using the GROMACS software package (Berendsen et al. 1995; Pronk et al. 2013; Van Der Spoel et al. 2005) version 4.5.3 on the π-supercomputer facility of SJTU (http://pi.sjtu.edu.cn/) with the CHARMM36 protein/lipid force field. The simulations were performed at constant temperature and pressure at 323 K and 1 atm, respectively, using a V-rescale thermostat (Bussi et al. 2007) and semi-isotropic Berendsen barostat, with coupling time constant of 0.1 and 1, respectively. A plane cutoff function was used for the calculation of non-bonded interactions with cutoff distance of 1.0 nm. PME was applied for the electrostatic calculations with a coulomb cutoff of 1.0 nm, Fourier spacing of 0.12 nm, and an interpolation order 4. Charge neutrality was ensured by adding Cl ions, because melittin has six positive charges, and a salt solution of 0.1 M NaCl was chosen. All bond lengths involving hydrogen atoms were held fixed using the LINCS algorithm. A Maxwell velocity distribution at 323 K was used for generating an initial velocity required to start the simulation. A time step of 2 fs was used. Each system was individually simulated at the time scale between 2.5 and 4.2 μs. Analysis and visualization were performed with GROMACS in built analysis tools and VMD (Humphrey et al. 1996), respectively.

Results and Discussion

To understand the mechanism of membrane disturbance by melittin at the molecular level, we performed five different atomistic simulations (Table 1) up to several μs with CHARMM36 protein/lipid force field into DMPC bilayers. The number of peptides/lipid molecules and the placement/orientations (Symmetric and asymmetric setup) of peptides on bilayers membranes varied in all simulations to make the system diverse and reproducible. Earlier, experimental studies (Matsuzaki et al. 1997; Vogel and Jahnig 1986) proposed that melittin binds to only one side of the bilayer (Asymmetric arrangements). However, a recent spectroscopic study (Lee et al. 2013) suggested a possible symmetric arrangement for melittin on the bilayer surface. Therefore, to understand the effect of symmetric and asymmetric arrangements of melittin on a bilayer and their possible role in membrane disruptions, four simulations, two in each condition, with varying numbers of peptide–lipid were performed (Table 1).

During the simulation time, we did not observe any spontaneous insertion of peptides from the membrane surface to a TM-inserted orientation; this despite our simulation being much longer than other reported studies of atomistic simulations. Such an insertion would require the translocation of at least one charged side chain from

Table 1 Summary of the simulated systems

Simulation	*P*/*L*	Total *P*/*L*, Side1/Side2/partly inserted	Number of Na/Cl ions	Number of waters	Time (μs)
1.	1:25	2/0/0	10/22	2874	3.8
2.	1:25	8/0/0	40/88	11,496	3.2
3.	1:25	1/1/0	10/22	2790	2.6
4.	1:25	4/4/0	40/88	11,160	3.2
5.	1:23	9/0/9	90/198	25,866	4.2

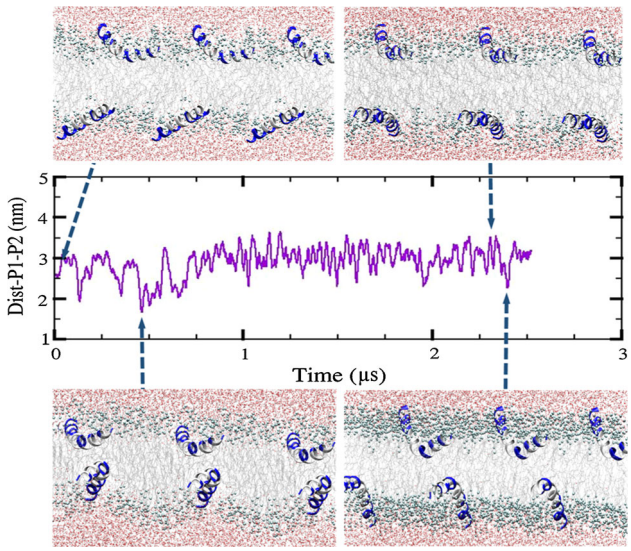

Fig. 1 Center of mass distance between two peptides during the simulation. Random snapshots of the conformational exchange between S-states and U-shaped conformations in system 3 are displayed. Polar and non-polar residues are shown in *blue* and *white*, respectively. Periodic images are shown to illustrate the box dimensions (Color figure online)

one bilayer leaflet to the other, a significant barrier to be overcome. In general, melittin buries quite deeply into the lipid bilayer, as shown in Fig. 3, with an average peptide center of mass 1.9 ± 0.4 Å below the lipid phosphates. Qualitatively, our results are in agreement with the X-ray/Neutron scattering experiments (Hristova et al. 2001), where author observed the location of melittin in the head group region of the bilayer.

However, we found the presence of bent U-shaped structures of peptides buried much deeper into the TM region (CM $\sim$ 2 Å from the bilayer center) in all simulations, irrespective of the system setup (Figs. 1, 2, 3). The exchange of the conformational states of melittin between U-shaped and parallel to membrane surface (S-state) was transient and several events were observed throughout the simulations in all setups. A longer lived state of the U-shaped conformation was observed for run four, with the participation of the peptides from both sides of the membrane (Fig. 2), with both their termini attached to the same bilayer leaflet. In a recent CG simulation study (Santo et al. 2013), it was reported that if a U-shaped conformation was formed by peptides from only one side of the membrane, it assisted pore formation. However, if the peptides participated from both sides of the membrane, they probably lost their wedge structures and did not help in pore formation. On the contrary, we did not observe any significant contribution by U-shaped conformations to facilitate pore formations in either case. In this conformation, both positively charged termini of melittin interact with negatively charged head group of lipids and facilitate the burial of hydrophobic residues into the hydrophobic core of the lipid bilayer. It clearly is a thermodynamically favorable conformation of melittin in lipid bilayers.

Whether the U-shaped conformation has some functional relevance in membrane disruption is unclear. The symmetric arrangements of double U-shaped structures are long lasting and stabilized by hydrogen bonds formed between THR10 and THR11 from both peptides (Fig. 2). Further, the presence of a few water bridges was always observed around these arrangements that may further contribute to stability. It is fairly possible that this arrangement might help in membrane collapsing when the pressure on either or both leaflets of the membrane reaches higher than a threshold value.

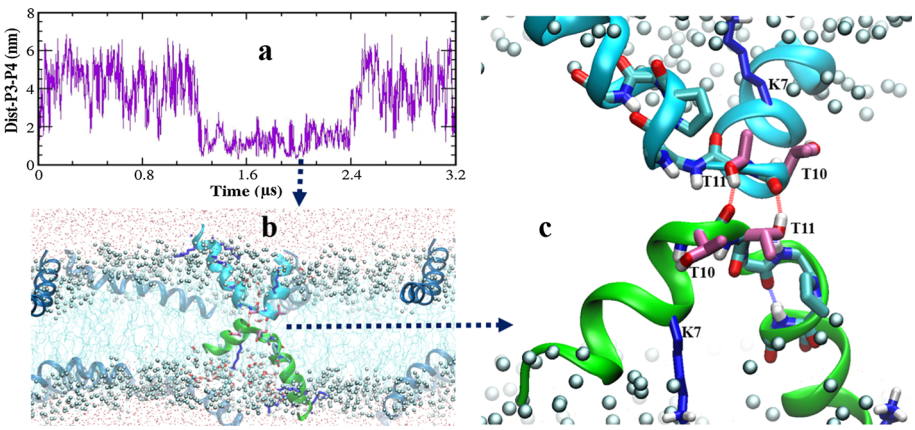

Fig. 2 **a** Center of mass (CM) distance with respect to simulation time between peptides 3 and 4, involved in the formation of a temporary U-shaped structure in symmetric arrangement. **b** Representative structure of U-shaped conformation, taken from the trajectory at 2.2 μs, indicated by a *blue arrow*. **c** Closer view of the U-shaped structure including details of residues involved in H-bond formation. The phosphate atoms of the lipid head groups are shown as *cyano spheres*, lysine side chains are shown in *blue*, and hydrogen bonds are shown as *dotted lines* (Color figure online)

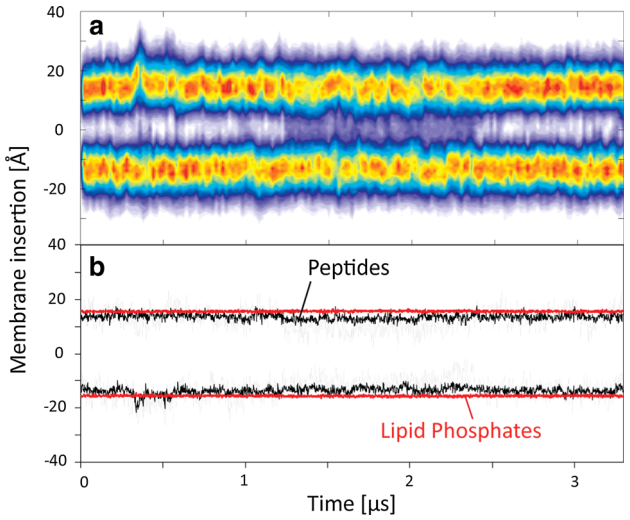

Fig. 3 **a** Normalized membrane peptide density profile of the symmetric simulation involving eight melittin peptides. **b** A plot of the center of mass (CM) of all peptides (*black*) in each leaflet shows that melittin is buried deeply into the interface, 1.9 Å below the lipid phosphate groups (*red*). For peptides 3 and 4, involved in the formation of a temporary U-shaped structure, the CM burial can be as deep as 2 Å from the bilayer center (*grey*) (Color figure online)

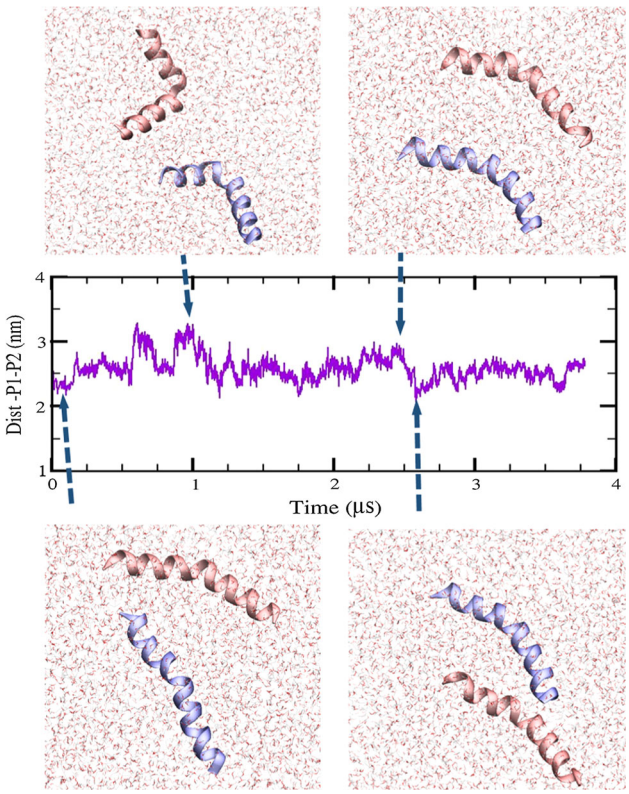

Fig. 5 The center of mass distance between two peptides in system-1 shows that the two peptides never come closer than 2 nm. Snapshots show the conformational states of the peptides at different time steps during the simulation. The exchange between S-states and bent U-shaped conformation can be seen in different snapshots

In the present study, we never observed an event where the center of mass of two peptides came closer than 2 nm (Figs. 4, 5), even in the case where several peptides were entirely anchored into TM positions along with surface arrangements (Fig. 6). This is expected because melittin carries a high positive charge density, and peptides are more likely to move apart from each other to reduce electrostatic repulsion and minimize the entropy, rather than taking part in the pore formation by the process of aggregations. If there is a possibility of pore formation by many peptides, it must be lined with several waters and the head group of lipids, and the pore size should be large enough to neutralize the effect of electrostatic repulsion. Yet, this has only been seen in simulation studies of melittin when the individual helices were arranged in a pre-assembled tetrameric toroidal pore; they repelled each other causing a disruption of the lipid bilayer within 4 ns due to the movement of one peptide apart from others (Lin and Baumgaertner 2000). However, it is most likely that if the simulation time is longer, then all peptides could move away to minimize the effect of electrostatic repulsion.

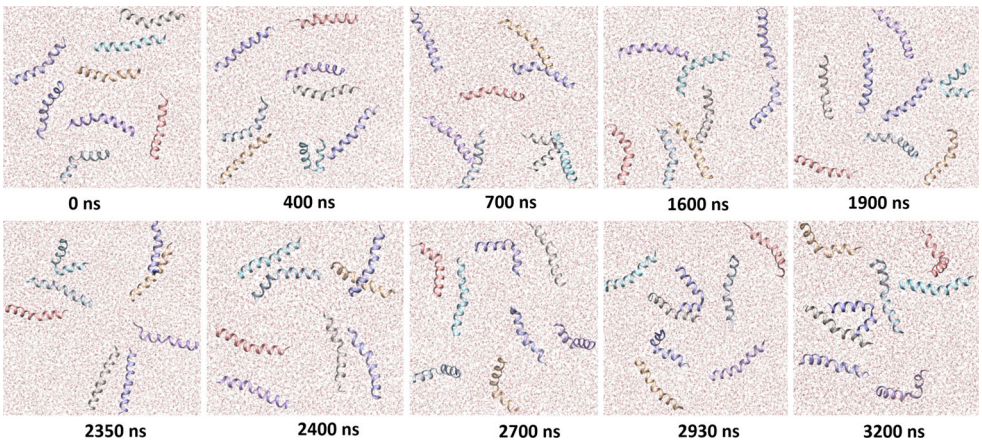

Fig. 4 Random snapshots of system-2 (asymmetric setup with eight peptides) at different simulation times. Note that the exchange of conformations between S-states and U-shaped conformation can be observed several times during simulation for different peptides. No peptide aggregation events are observed during simulation time of 3.2 μs

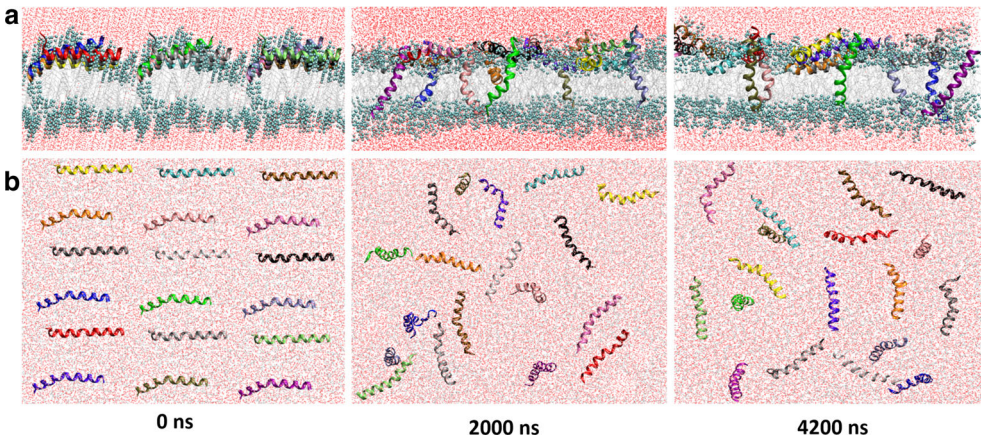

Fig. 6 Initial setup (0 ns) with partially inserted peptides in an artificially created water pore, lined with lipid head groups, along with other snapshots during the simulation time is shown in **a** (*side view*) and **b** (*top view*), respectively. The artificially created pore disappeared quickly after peptide translocation. No further pores and no aggregation events are observed up to 4.2-μs simulation

In the absence of spontaneous insertion of melittin peptides from the membrane surface to TM orientations, or of pore formation, we performed another simulation with 18 peptides in 414 DMPC lipids (Table 1). This simulation started with half of the peptides partially inserted parallel to the membrane axis within an artificially created water defect spanning the membrane with tilted peptides. In the initial arrangement, nine peptides were half inserted in TM in artificially created pores and others were laid parallel to the membrane surface (Fig. 6). All peptides were initially equally distanced. During the simulation, six of the nine peptides were completely inserted and aligned parallel to the membrane normal within 20 ns, with the other three reverting back to the membrane surface. Once the peptides got inserted into the membrane, the artificially created pores quickly disappeared and we did not observe any aggregations, insertions or further pore formation events up to 4.2 μs simulated trajectory. The apparent instability of the transient, non-equilibrium initial water pore structure indicates that membrane defects involving single melittin peptides are highly unlikely, and that aggregation is essential. Unfortunately, no equilibrium pore formation could be observed even for such partially inserted simulations.

Conclusions

The mechanism of membrane perturbation by melittin remains puzzling. In a previous 17-μs-long study in DOPC, melittin remained firmly locked into horizontal surface aligned states at low *P*/*L* (Andersson et al. 2013). Here, we have substantially increased the *P*/*L* ratio and have used a thinner bilayer (DMPC). However, still neither peptide insertion nor pore formation is observed over 3–4 μs. This contrasts with some prior simulation studies on related AMPs (Irudayam and Berkowitz 2011; Leontiadou et al. 2006; Manna and Mukhopadhyay 2009; Sengupta et al. 2008), where pore formation was observed in only a few tens of nanoseconds, ~100 times shorter than our simulations here. We have recently shown that simulations of AMPs can be poorly converged and depend highly on the chosen force field (Wang et al. 2014), so these earlier results are likely biased toward specific initial arrangement or incorrect.

Instead of pores, we find metastable bent U-shaped conformations spanning the membrane, involving two melittin peptides from both sides of the membrane. These structures require that at least one peptide has translocated however. It appears that the only way to insert melittin into a TM orientation, or to induce water pores, is to start from highly non-equilibrium pre-inserted conformations, where key charged sidechains are already pointing to the opposing bilayer leaflet. Unfortunately, this defeats the goal of using unbiased simulations in predicting AMP activity.

Even if melittin peptides are already inserted in TM orientations, it is challenging to predict the structure of pores in reasonable computational time: In a recent MD study, four melittin peptides were inserted into a TM orientation in both zwitterionic and anionic bilayers, and the system equilibrated for 9 μs, about 3 times longer than the simulations presented here (Leveritt 2015). Very little structural change was observed even for this case. Unfortunately, pre-assembled structures do not allow for an unbiased prediction of how many peptides are actually involved in a melittin pore, or whether the peptides are aligned parallel or anti-parallel in such an arrangement. Clearly, membrane insertion and pore formation of melittin will require much longer timescales than ~10 μs and are more challenging than initially thought.

Acknowledgments This research was supported by a grant from the National Natural Science Foundation of China (91230105) and a 1000 Plan's Program for Young Talents (13Z127060001) to J.P.U.

References

Allende D, Simon SA, McIntosh TJ (2005) Melittin-induced bilayer leakage depends on lipid material properties: evidence for toroidal pores. Biophys J 88:1828–1837

Andersson M, Ulmschneider JakobP, Ulmschneider MartinB, White StephenH (2013) Conformational states of melittin at a bilayer interface. Biophys J 104:L12–L14

Berendsen HJC, van der Spoel D, van Drunen R (1995) GROMACS: a message-passing parallel molecular dynamics implementation. Comput Phys Commun 91:43–56

Berneche S, Nina M, Roux B (1998) Molecular dynamics simulation of melittin in a dimyristoylphosphatidylcholine bilayer membrane. Biophys J 75:1603–1618

Brogden KA (2005) Antimicrobial peptides: pore formers or metabolic inhibitors in bacteria? Nat Rev Microbiol 3:238–250

Brown KL, Hancock RE (2006) Cationic host defense (antimicrobial) peptides. Curr Opin Immunol 18:24–30

Brown LR, Lauterwein J, Wuthrich K (1980) High-resolution 1H-NMR studies of self-aggregation of melittin in aqueous solution. Biochim Biophys Acta 622:231–244

Bussi G, Donadio D, Parrinello M (2007) Canonical sampling through velocity rescaling. J Chem Phys 126:014101

Chen X, Wang J, Boughton AP, Kristalyn CB, Chen Z (2007) Multiple orientation of melittin inside a single lipid bilayer determined by combined vibrational spectroscopic studies. J Am Chem Soc 129:1420–1427

Chromek M, Slamova Z, Bergman P, Kovacs L, Podracka L, Ehren I, Hokfelt T, Gudmundsson GH, Gallo RL, Agerberth B, Brauner A (2006) The antimicrobial peptide cathelicidin protects the urinary tract against invasive bacterial infection. Nat Med 12:636–641

Demchenko AP, Kostrzhevskaia EG (1986) Melittin: structure, properties, interaction with a membrane. Ukr Biokhim Zh 58:92–103

Hancock RE, Scott MG (2000) The role of antimicrobial peptides in animal defenses. Proc Natl Acad Sci USA 97:8856–8861

Hristova K, Dempsey CE, White SH (2001) Structure, location, and lipid perturbations of melittin at the membrane interface. Biophys J 80(2):801–811

Huang HW (2000) Action of antimicrobial peptides: two-state model. Biochemistry 39:8347–8352

Humphrey W, Dalke A, Schulten K (1996) VMD: visual molecular dynamics. J Mol Graph 14(33–8):27–28

Irudayam SJ, Berkowitz ML (2011) Influence of the arrangement and secondary structure of melittin peptides on the formation and stability of toroidal pores. Biochim Biophys Acta 1808:2258–2266

Irudayam SJ, Berkowitz ML (2012) Binding and reorientation of melittin in a POPC bilayer: computer simulations. Biochim Biophys Acta 1818:2975–2981

Iwadate M, Asakura T, Williamson MP (1998) The structure of the melittin tetramer at different temperatures—an NOE-based calculation with chemical shift refinement. Eur J Biochem 257:479–487

Langham AA, Ahmad AS, Kaznessis YN (2008) On the nature of antimicrobial activity: a model for protegrin-1 pores. J Am Chem Soc 130:4338–4346

Lee MT, Sun TL, Hung WC, Huang HW (2013) Process of inducing pores in membranes by melittin. Proc Natl Acad Sci USA 110:14243–14248

Leontiadou H, Mark AE, Marrink SJ (2006) Antimicrobial peptides in action. J Am Chem Soc 128:12156–12161

Leveritt JM III (2015) The structure of a melittin-stabilized toroidal pore. Biophys J 108(2):249a. doi:10.1016/j.bpj.2014.11.1380

Lin JH, Baumgaertner A (2000) Stability of a melittin pore in a lipid bilayer: a molecular dynamics study. Biophys J 78:1714–1724

Lohner K, Blondelle SE (2005) Molecular mechanisms of membrane perturbation by antimicrobial peptides and the use of biophysical studies in the design of novel peptide antibiotics. Comb Chem High Throughput Screen 8:241–256

Manna M, Mukhopadhyay C (2009) Cause and effect of melittin-induced pore formation: a computational approach. Langmuir 25:12235–12242

Matsuzaki K, Yoneyama S, Miyajima K (1997) Pore formation and translocation of melittin. Biophys J 73:831–838

Park Y, Hahm KS (2005) Antimicrobial peptides (AMPs): peptide structure and mode of action. J Biochem Mol Biol 38:507–516

Pronk S, Pall S, Schulz R, Larsson P, Bjelkmar P, Apostolov R, Shirts MR, Smith JC, Kasson PM, van der Spoel D, Hess B, Lindahl E (2013) GROMACS 4.5: a high-throughput and highly parallel open source molecular simulation toolkit. Bioinformatics 29:845–854

Rex S (1996) Pore formation induced by the peptide melittin in different lipid vesicle membranes. Biophys Chem 58(1–2):75–85

Sanchez-Martinez S, Huarte N, Maeso R, Madan V, Carrasco L, Nieva JL (2008) Functional and structural characterization of 2B viroporin membranolytic domains. Biochemistry 47:10731–10739

Santo KP, Irudayam SJ, Berkowitz ML (2013) Melittin creates transient pores in a lipid bilayer: results from computer simulations. J Phys Chem B 117:5031–5042

Schwarz G, Zong RT, Popescu T (1992) Kinetics of melittin induced pore formation in the membrane of lipid vesicles. Biochim Biophys Acta 1110(1):97–104

Sengupta D, Leontiadou H, Mark AE, Marrink SJ (2008) Toroidal pores formed by antimicrobial peptides show significant disorder. Biochim Biophys Acta 1778:2308–2317

Sharon M, Oren Z, Shai Y, Anglister J (1999) 2D-NMR and ATR-FTIR study of the structure of a cell-selective diastereomer of melittin and its orientation in phospholipids. Biochemistry 38:15305–15316

Son DJ, Lee JW, Lee YH, Song HS, Lee CK, Hong JT (2007) Therapeutic application of anti-arthritis, pain-releasing, and anti-cancer effects of bee venom and its constituent compounds. Pharmacol Ther 115:246–270

van den Bogaart G, Guzman JV, Mika JT, Poolman B (2008) On the mechanism of pore formation by melittin. J Biol Chem 283:33854–33857

Van Der Spoel D, Lindahl E, Hess B, Groenhof G, Mark AE, Berendsen HJ (2005) GROMACS: fast, flexible, and free. J Comput Chem 26:1701–1718

Vogel H, Jahnig F (1986) The structure of melittin in membranes. Biophys J 50:573–582

Wang Y, Zhao T, Wei D, Strandberg E, Ulrich AS, Ulmschneider JP (2014) How reliable are molecular dynamics simulations of membrane active antimicrobial peptides? Biochim Biophys Acta Biomembr 1838:2280–2288

Yang L, Harroun TA, Weiss TM, Ding L, Huang HW (2001) Barrel-stave model or toroidal model? A case study on melittin pores. Biophys J 81:1475–1485

Yeaman MR, Yount NY (2003) Mechanisms of antimicrobial peptide action and resistance. Pharmacol Rev 55:27–55

Zhu L, Kemple MD, Yuan P, Prendergast FG (1995) N-terminus and lysine side chain pKa values of melittin in aqueous solutions and micellar dispersions measured by 15 N NMR. Biochemistry 34:13196–13202